Available online at www.sciencedirect.com
SCIENCE DIRECT®
Journal of Sound and Vibration 289 (2006) 871–888
JOURNAL OF SOUND AND VIBRATION
www.elsevier.com/locate/jsvi

Wave attenuation in nonlinear periodic structures using harmonic balance and multiple scales

Amol Marathe*, Anindya Chatterjee

Mechanical Engineering, Indian Institute of Science, Bangalore 560012, India

Received 31 March 2004; received in revised form 17 February 2005; accepted 23 February 2005
Available online 8 August 2005

Abstract

We study the attenuation, caused by weak damping, of harmonic waves through a discrete, periodic structure with frequency nominally within the Propagation Zone (i.e., propagation occurs in the absence of the damping). The period of the structure consists of a linear stiffness and a weak linear/nonlinear damping. Adapting the transfer matrix method and using harmonic balance for the nonlinear terms, a four-dimensional linear/nonlinear map governing the dynamics is obtained. We analyze this map by applying the method of multiple scales upto first order. The resulting slow evolution equations give the amplitude decay rate in the structure. The approximations are validated by comparing with other analytical solutions for the linear case and full numerics for the nonlinear case. Good agreement is obtained. The method of analysis presented here can be extended to more complex structures.

1. Introduction

Periodic structures occur often in nature and engineering. Atomic lattices of pure crystals are examples found in nature. Multistoreyed buildings, elevated guideways for high-speed transportation vehicles, multispan bridges, bladed disk assemblies in turbines, and stiffened shells in aircraft and ships provide examples in engineering.

*Corresponding author.
E-mail addresses: amol@mecheng.iisc.ernet.in (A. Marathe), anindya@mecheng.iisc.ernet.in (A. Chatterjee).

0022-460X/$ - see front matter © 2005 Elsevier Ltd. All rights reserved.
doi:10.1016/j.jsv.2005.02.047

The problem of wave propagation in periodic structures has received significant attention over the last four decades (see, e.g., Ref. [1]). The vast majority of papers on this topic have dealt with linear structures. There exists a large body of work on linear periodic structures. A beginning reader is referred to Mead's excellent review [1] and references therein. Significant contributions may also be found in, e.g., Refs. [2–6] (the list is incomplete, but representative). In this paper, we study wave propagation in nonlinear periodic structures using harmonic balance and multiple scales.

The main issues in the linear case can be outlined in the context of the structure sketched in Fig. 1. Assume zero damping and linear stiffness. If one end of a semi-infinite periodic structure is excited at a frequency ω then, lack of dissipation notwithstanding, a steady wave may fail to propagate with undiminished amplitude. Bands of frequencies in which waves do propagate with undiminished amplitude are called *propagation zones* (PZ). Bands where the amplitude diminishes are called *attenuation zones* (AZ). The number of distinct PZs equals the number of degrees of freedom of one period of the structure [1]. The *propagation constant* for a wave at a given frequency is the logarithm of the ratio of complex amplitudes of vibrations of successive elements. The real part of the propagation constant is called the attenuation constant and the imaginary part is called the phase constant. Zero attenuation corresponds to PZs while nonzero attenuation corresponds to AZs. Though propagation constants are most meaningful for linear structures (damped or undamped), a useful interpretation is possible in the case of propagating waves in weakly nonlinear but conservative periodic structures [7].

The literature on harmonic wave propagation through weakly nonlinear periodic structures, in comparison to linear structures, is meagre. A likely reason is that the powerful and popular matrix-based approaches in the frequency domain used for linear periodic structures run into trouble in the presence of nonlinearities. Recently, Mallik and Chakraborty have studied *conservative* weakly nonlinear periodic structures [7]. They used single-frequency harmonic balance to describe the nonlinear behavior of a single period of the structure in the frequency domain, and developed a simple, amplitude-dependent, perturbation expansion of the propagation constant to elucidate several aspects of wave propagation phenomena in the presence of weak, conservative nonlinearities. However, they did not address damping (linear or nonlinear).

In this paper, we consider a weakly nonlinear, *damped* periodic structure. Using Mallik and Chakraborty's idea of harmonic balance in the periodic structures context, we obtain a weakly nonlinear map (as opposed to simply a transfer matrix) that approximately governs the wave propagation in such a structure. The propagation zones of the undamped structure now become zones of weak attenuation. We then use the method of multiple scales (MMS) for maps to study the weak attenuation in our structure. Note that the MMS for maps is not new [8–10]; its use for wave propagation in periodic structures is new, however. Our approach can also be used for other

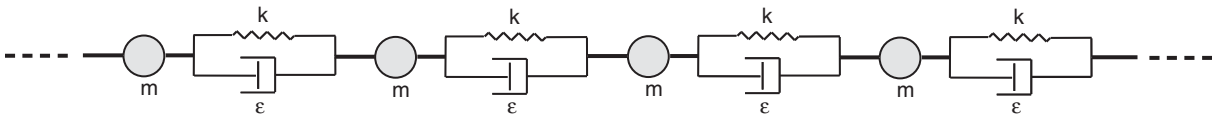

Fig. 1. A periodic structure.

small perturbations to linear periodic structures within propagation zones, including conservative nonlinearities.

2. Weakly damped periodic structures

We will study the cases of linear and nonlinear damping along similar lines.

2.1. Linear damping

Consider the nth element E_n of a periodic structure consisting, for greatest simplicity, of a mass m, a linear spring of stiffness k, and a weak damper of coefficient ε (see Fig. (2)). We assume $0<\varepsilon\ll 1$. Successive elements interact through displacement and force at connecting points, as indicated. For linear damping, the damping force is $\varepsilon(\dot{X}_n-\dot{X}_{n+1})$. Applying force and momentum balance on the nth element, and assuming a harmonic solution, we write

$$X_n = X_{n,c}\cos(\omega t) + X_{n,s}\sin(\omega t), \tag{1a}$$

$$F_n = F_{n,c}\cos(\omega t) + F_{n,s}\sin(\omega t). \tag{1b}$$

The governing equations can be written in the following matrix form:

$$\begin{Bmatrix} X_{n+1,c} \\ X_{n+1,s} \\ F_{n+1,c} \\ F_{n+1,s} \end{Bmatrix} = \begin{bmatrix} 1-\dfrac{m\omega^2 k}{\varepsilon^2\omega^2+k^2} & \dfrac{m\omega^3\varepsilon}{\varepsilon^2\omega^2+k^2} & -\dfrac{k}{\varepsilon^2\omega^2+k^2} & \dfrac{\varepsilon\,\omega}{\varepsilon^2\omega^2+k^2} \\ -\dfrac{m\omega^3\varepsilon}{\varepsilon^2\omega^2+k^2} & 1-\dfrac{m\omega^2 k}{\varepsilon^2\omega^2+k^2} & -\dfrac{\varepsilon\,\omega}{\varepsilon^2\omega^2+k^2} & -\dfrac{k}{\varepsilon^2\omega^2+k^2} \\ m\omega^2 & 0 & 1 & 0 \\ 0 & m\omega^2 & 0 & 1 \end{bmatrix} \begin{Bmatrix} X_{n,c} \\ X_{n,s} \\ F_{n,c} \\ F_{n,s} \end{Bmatrix}. \tag{2}$$

The above equation is of the form

$$\mathbf{q}_{n+1} = \mathbf{T}\mathbf{q}_n. \tag{3}$$

By definition, an eigenvalue σ of matrix $\mathbf{T}$ and the associated propagation constant μ are related by

$$\sigma = \mathrm{e}^{-\mu}. \tag{4}$$

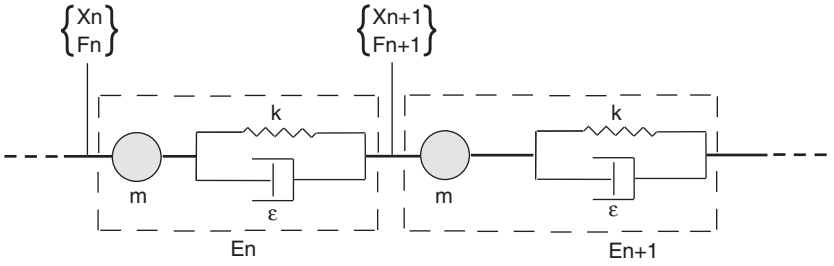

Fig. 2. Successive elements of the periodic structure.

Numerical results showing μ versus ω will be presented later (see Fig. 4). First, we develop a small ε approximation that will work for the nonlinear case as well.

Eq. (2) can also be written as

$$\begin{Bmatrix} X_{n+1,c} \\ X_{n+1,s} \\ F_{n+1,c} \\ F_{n+1,s} \end{Bmatrix} = \begin{bmatrix} 1-\dfrac{m\omega^2}{k} & 0 & -\dfrac{1}{k} & 0 \\ 0 & 1-\dfrac{m\omega^2}{k} & 0 & -\dfrac{1}{k} \\ m\omega^2 & 0 & 1 & 0 \\ 0 & m\omega^2 & 0 & 1 \end{bmatrix} \begin{Bmatrix} X_{n,c} \\ X_{n,s} \\ F_{n,c} \\ F_{n,s} \end{Bmatrix} + \varepsilon \frac{\omega}{k} \begin{Bmatrix} \dfrac{m\omega^2 X_{n,s} + F_{n,s}}{k} \\ -\dfrac{m\omega^2 X_{n,c} + F_{n,c}}{k} \\ 0 \\ 0 \end{Bmatrix} + \mathcal{O}(\varepsilon^2). \tag{5}$$

Neglecting $\mathcal{O}(\varepsilon^2)$ terms, Eq. (5) is of the form

$$\mathbf{q}_{n+1} = \mathbf{B}\mathbf{q}_n + \varepsilon \mathbf{L}(\mathbf{q}_n). \tag{6}$$

2.2. Nonlinear damping

We now take the damping force to be $\varepsilon(\dot{X}_n - \dot{X}_{n+1})^3$ (cubic nonlinearity). Using Eqs. (1), but now in a one-term harmonic balance approximation, we obtain the governing equations in the form

$$\mathbf{q}_{n+1} = \mathbf{B}\mathbf{q}_n + \varepsilon \mathbf{N}(\mathbf{q}_n), \tag{7}$$

with $\mathbf{B}$ and $\mathbf{q}_n$ the same as in the linear damping case, and with $\mathbf{N}(\mathbf{q}_n)$ given by

$$\mathbf{N}(\mathbf{q}_n) = \frac{3}{4}\left(\frac{\omega}{k}\right)^3 \left\{ \left(m\omega^2 X_{n,c} + F_{n,c}\right)^2 + \left(m\omega^2 X_{n,s} + F_{n,s}\right)^2 \right\} \begin{Bmatrix} \dfrac{m\omega^2 X_{n,s} + F_{n,s}}{k} \\ -\dfrac{m\omega^2 X_{n,c} + F_{n,c}}{k} \\ 0 \\ 0 \end{Bmatrix}. \tag{8}$$

3. Method of multiple scales

A method of multiple scales for two-dimensional maps has been presented in, e.g., Refs. [8–10]. For completeness, we briefly present the method for the system

$$\mathbf{q}_{n+1} = \mathbf{A}\mathbf{q}_n + \varepsilon \mathbf{N}(\mathbf{q}_n) \tag{9}$$

with $0 < \varepsilon \ll 1$ and

$$\mathbf{q}_n = \begin{Bmatrix} q_{n,1} \\ q_{n,2} \end{Bmatrix}.$$

The method, as used here, assumes that **A** has a pair of strictly complex conjugate eigenvalues of unit magnitude. Although Eqs. (6) and (7) are four-dimensional maps, the method of analysis is similar.

For our two-dimensional map, we take

$$\mathbf{A} = \begin{bmatrix} \frac{1}{\sqrt{2}} & \frac{1}{\sqrt{2}} \\ -\frac{1}{\sqrt{2}} & \frac{1}{\sqrt{2}} \end{bmatrix} \quad \text{and} \quad \mathbf{N}(\mathbf{q}_n) = (q_{n,1}^2 + q_{n,2}^2) \begin{Bmatrix} -q_{n,1} - q_{n,2} \\ 2\,q_{n,1} \end{Bmatrix}. \tag{10}$$

The eigenvalues σ, $\bar{\sigma}$ of **A** are

$$\sigma = \frac{1+\mathrm{i}}{\sqrt{2}}, \quad \bar{\sigma} = \frac{1-\mathrm{i}}{\sqrt{2}}.$$

The right eigenvectors ($\mathbf{u}$, $\bar{\mathbf{u}}$) and left eigenvectors ($\boldsymbol{\xi}, \bar{\boldsymbol{\xi}}$) correspondng to the eigenvalues σ, $\bar{\sigma}$ are

$$\mathbf{u} = \begin{Bmatrix} u_1 \\ u_2 \end{Bmatrix} = \begin{Bmatrix} \frac{1}{\sqrt{2}} \\ \frac{\mathrm{i}}{\sqrt{2}} \end{Bmatrix}, \quad \bar{\mathbf{u}} = \begin{Bmatrix} \bar{u}_1 \\ \bar{u}_2 \end{Bmatrix} = \begin{Bmatrix} \frac{1}{\sqrt{2}} \\ -\frac{\mathrm{i}}{\sqrt{2}} \end{Bmatrix}, \tag{11a}$$

$$\boldsymbol{\xi} = \begin{Bmatrix} \xi_1 & \xi_2 \end{Bmatrix} = \begin{Bmatrix} \frac{1}{\sqrt{2}} & \frac{\mathrm{i}}{\sqrt{2}} \end{Bmatrix}, \quad \bar{\boldsymbol{\xi}} = \begin{Bmatrix} \bar{\xi}_1 & \bar{\xi}_2 \end{Bmatrix} = \begin{Bmatrix} \frac{1}{\sqrt{2}} & -\frac{\mathrm{i}}{\sqrt{2}} \end{Bmatrix}. \tag{11b}$$

We assume that the solution to Eq. (9) depends upon two independent scales, n (fast) and $s = \varepsilon n$ (slow). We assume further that the solution can be expanded as [8]

$$\mathbf{q}_n = \mathbf{Q}(n,s) = \mathbf{Q}_0(n,s) + \varepsilon\,\mathbf{Q}_1(n,s) + \mathcal{O}(\varepsilon^2), \tag{12}$$

$$\mathbf{q}_{n+1} = \mathbf{Q}(n+1, s+\varepsilon) = \mathbf{Q}_0(n+1, s+\varepsilon) + \varepsilon\mathbf{Q}_1(n+1, s+\varepsilon) + \mathcal{O}(\varepsilon^2). \tag{13}$$

We also assume that the **Q**s in Eqs. (12) and (13) vary smoothly with s. Then (as in Ref. [10])

$$\mathbf{q}_{n+1} = \mathbf{Q}(n+1, s+\varepsilon) = \mathbf{Q}_0(n+1, s) + \varepsilon[\mathbf{Q}_1(n+1, s) + \partial_s \mathbf{Q}_0(n+1, s)] + \mathcal{O}(\varepsilon^2), \tag{14}$$

where ∂_s denotes a partial derivative with respect to s. Substituting Eqs. (12) and (14) into Eq. (9), we obtain

$$\mathbf{Q}_0(n+1,s) + \varepsilon[\mathbf{Q}_1(n+1,s) + \partial_s \mathbf{Q}_0(n+1,s)] = \mathbf{A}\mathbf{Q}_0(n,s) + \varepsilon\mathbf{A}\mathbf{Q}_1(n,s) + \mathbf{N}(\mathbf{Q}_0(n,s)) + \mathcal{O}(\varepsilon^2). \tag{15}$$

At $\mathcal{O}(1)$:

$$\mathbf{Q}_0(n+1,s) = \mathbf{A}\mathbf{Q}_0(n,s). \tag{16}$$

The general solution to Eq. (16), for arbitrary n, is

$$\mathbf{Q}_0(n,s) = \alpha(s)\sigma^n \mathbf{u} + \bar{\alpha}(s)\bar{\sigma}^n \bar{\mathbf{u}}, \tag{17}$$

where $\alpha(s)$ and $\bar{\alpha}(s)$ are arbitrary, differentiable functions of s. It follows that

$$\partial_s \mathbf{Q}_0(n+1,s) = \partial_s \alpha \sigma^{n+1}\mathbf{u} + \partial_s \bar{\alpha}\bar{\sigma}^{n+1}\bar{\mathbf{u}}. \tag{18}$$

Using Eq. (17), $\mathbf{N}(\mathbf{Q}_0(n,s))$ in Eq. (15) will now be written, for arbitrary n, as

$$\mathbf{N}(\mathbf{Q}_0(n,s)) = \sum_{k=-M}^{M} \mathbf{c}_k \sigma^{kn} \tag{19}$$

for some finite integer M and appropriate vectors $\mathbf{c}_k$, each independent of σ and $\bar{\sigma}$. With Eqs. (18) and (19), we then get at $\mathcal{O}(\varepsilon)$:

$$\mathbf{Q}_1(n+1,s) - \mathbf{A}\mathbf{Q}_1(n,s) = (-\partial_s \alpha \sigma \mathbf{u} + \mathbf{c}_1)\sigma^n + (-\partial_s \bar{\alpha}\bar{\sigma}\bar{\mathbf{u}} + \mathbf{c}_{-1})\bar{\sigma}^n + \text{ other powers}, \tag{20}$$

where the 'other powers' do not cause resonances and associated secular terms. For the example considered,

$$\mathbf{c}_1 = \alpha(s)^2\bar{\alpha}(s)\begin{Bmatrix} -3(\bar{u}_1 u_1^2 + \bar{u}_2 u_2^2) - 2(\bar{u}_1 + \bar{u}_2)u_1 u_2 - (u_1^2\bar{u}_2 + u_2^2\bar{u}_1) \\ 3u_1^2\bar{u}_1 + 2u_1 u_2 \bar{u}_2 + \bar{u}_1 u_2^2 \end{Bmatrix} \quad \text{and} \quad \mathbf{c}_{-1} = \bar{\mathbf{c}}_1. \tag{21}$$

To remove the secular terms (which process lies at the heart of the multiple scales method), the coefficient vectors of σ^n and $\bar{\sigma}^n$ should be orthogonal to the left eigenvectors of $\mathbf{A}$ corresponding to the eigenvalues σ and $\bar{\sigma}$, respectively; these two conditions may also be looked upon as solvability conditions that yield the slow evolution sought here. These conditions are

$$-\partial_s \alpha \sigma \boldsymbol{\xi}\mathbf{u} + \boldsymbol{\xi}\mathbf{c}_1 = 0, \tag{22a}$$

$$-\partial_s \bar{\alpha}\bar{\sigma}\bar{\boldsymbol{\xi}}\bar{\mathbf{u}} + \bar{\boldsymbol{\xi}}\mathbf{c}_{-1} = 0. \tag{22b}$$

From Eqs. (11a), (21) and (22), we obtain

$$\partial_s \alpha = -(2+i)\sqrt{2}\bar{\alpha}(s)\alpha^2(s), \tag{23a}$$

$$\partial_s \bar{\alpha} = -(2-i)\sqrt{2}\alpha(s)\bar{\alpha}^2(s). \tag{23b}$$

Approximating

$$\partial_s \alpha \approx \frac{\alpha(s+\varepsilon) - \alpha(s)}{\varepsilon} = \frac{\alpha_{n+1} - \alpha_n}{\varepsilon},$$

we can convert Eq. (23a) into the map:

$$\alpha_{n+1} = \alpha_n - \varepsilon(2+i)\sqrt{2}\bar{\alpha}_n \alpha_n^2. \tag{24}$$

For comparison, the oscillatory first component $q_{n,1}$ as obtained from direct numerical solution of the full map with $\varepsilon = 0.03$ is plotted in Fig. 3. In this case, the initial condition was randomly chosen to be

$$\mathbf{q}_0 = \begin{Bmatrix} 0.8318 \\ 0.5028 \end{Bmatrix}.$$

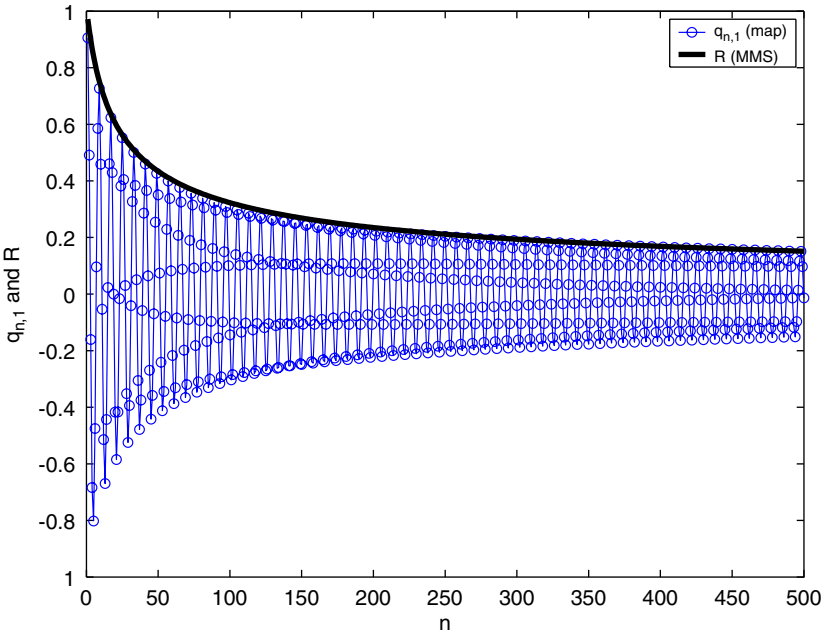

Fig. 3. Comparison between the numerical solution of Eq. (9) and the amplitude obtained by the MMS, Eq. (25) for $\varepsilon = 0.03$.

The solution for Eq. (24) was computed with the corresponding initial condition $\alpha_0 = 0.1648 - 0.6673i$. Note that the amplitude of $q_{n,1}$ is

$$R = \sqrt{2}\,|\alpha_n|. \tag{25}$$

The match between R and $q_{n,1}$ is excellent (see Fig. 3).

4. MMS for the linearly damped periodic structure

Consider Eq. (5), written as

$$\mathbf{q}_{n+1} = \mathbf{B}\mathbf{q}_n + \varepsilon \mathbf{L}(\mathbf{q}_n) \tag{26}$$

with $\mathbf{q}_n = \{X_{n,c} \quad X_{n,s} \quad F_{n,c} \quad F_{n,s}\}^{\mathrm{T}}$, where T denotes transpose. Here $\mathbf{B}$ is a 4×4 matrix having eigenvalues σ and $\bar{\sigma}$ with multiplicity two each. Taking the parameter values $k = 1$ and $m = 1$, we get

$$\sigma = 1 - \tfrac{1}{2}\omega^2 + \tfrac{1}{2}\sqrt{-4\omega^2 + \omega^4}.$$

The frequency range considered is $0<\omega<2$, for which the eigenvalues are strictly complex with unit magnitude. The right eigenvectors are now $\mathbf{u}$, $\mathbf{v}$ with

$$\mathbf{u}=\frac{\omega}{2\sqrt{1+\omega^2}}\begin{Bmatrix}\dfrac{\sqrt{4-\omega^2}}{\omega}\mathrm{i}-1\\0\\2\\0\end{Bmatrix}, \tag{27a}$$

$$\mathbf{v}=\frac{\omega}{2\sqrt{1+\omega^2}}\begin{Bmatrix}0\\\dfrac{\sqrt{4-\omega^2}}{\omega}\mathrm{i}-1\\0\\2\end{Bmatrix} \tag{27b}$$

and their complex conjugates $\bar{\mathbf{u}}$ and $\bar{\mathbf{v}}$. Similarly, the left eigenvectors are $\boldsymbol{\xi}, \boldsymbol{\eta}$ with

$$\boldsymbol{\xi}=\frac{\omega}{2\sqrt{1+\omega^2}}\begin{Bmatrix}-\dfrac{\mathrm{i}\omega}{2\sqrt{4-\omega^2}} & 0 & \dfrac{\omega}{\sqrt{4-\omega^2}}+\mathrm{i}0\end{Bmatrix}, \tag{28a}$$

$$\boldsymbol{\eta}=\frac{\omega}{2\sqrt{1+\omega^2}}\begin{Bmatrix}0 & -\dfrac{\mathrm{i}\omega}{2\sqrt{4-\omega^2}} & 0 & \dfrac{\omega}{\sqrt{4-\omega^2}}+\mathrm{i}\end{Bmatrix} \tag{28b}$$

and their complex conjugates $\bar{\boldsymbol{\xi}}$, $\bar{\boldsymbol{\eta}}$.

As before, we assume

$$\mathbf{q}_n=\mathbf{Q}(n,s)=\mathbf{Q}_0(n,s)+\varepsilon\mathbf{Q}_1(n,s)+\mathcal{O}(\varepsilon^2), \tag{29}$$

$$\mathbf{q}_{n+1}=\mathbf{Q}(n+1,s+\varepsilon)=\mathbf{Q}_0(n+1,s+\varepsilon)+\varepsilon\mathbf{Q}_1(n+1,s+\varepsilon)+\mathcal{O}(\varepsilon^2). \tag{30}$$

Substituting Eqs. (29) and (30) into Eq. (26) and collecting terms at $\mathcal{O}(1)$ gives

$$\mathbf{Q}_0(n+1,s)=\mathbf{B}\mathbf{Q}_0(n,s), \tag{31}$$

the solution to which is

$$\mathbf{Q}_0(n,s)=(\alpha(s)\mathbf{u}+\gamma(s)\mathbf{v})\sigma^n+(\bar{\alpha}(s)\bar{\mathbf{u}}+\bar{\gamma}(s)\bar{\mathbf{v}})\bar{\sigma}^n, \tag{32}$$

where $\alpha(s)$, $\gamma(s)$ are arbitrary, differentiable functions of s. Using Eq. (32), $\mathbf{L}(\mathbf{Q}_0(n,s))$ can be written as (see Eq. (19); here $M=1$)

$$\mathbf{L}(\mathbf{Q}_0(n,s))=\mathbf{c}_1\sigma^n+\mathbf{c}_{-1}\bar{\sigma}^n, \tag{33}$$

$$\mathbf{c}_1=\begin{Bmatrix}-\omega^3(\alpha(s)u_2+\gamma(s)v_2)-\omega(\alpha(s)u_4+\gamma(s)v_4)\\\omega^3(\alpha(s)u_1+\gamma(s)v_1)+\omega(\alpha(s)u_3+\gamma(s)v_3)\\0\\0\end{Bmatrix} \quad \text{and} \quad \mathbf{c}_{-1}=\bar{\mathbf{c}}_1, \tag{34}$$

where u_i's and v_i's are components of $\mathbf{u}$ and $\mathbf{v}$ given by Eq. (27). Eliminating the secular terms,

$$\boldsymbol{\xi}(-\partial_s\alpha\sigma\mathbf{u} - \partial_s\gamma\sigma\mathbf{v} + \mathbf{c}_1) = 0, \tag{35a}$$

$$\boldsymbol{\eta}(-\partial_s\alpha\sigma\mathbf{u} - \partial_s\gamma\sigma\mathbf{v} + \mathbf{c}_1) = 0, \tag{35b}$$

$$\bar{\boldsymbol{\xi}}(-\partial_s\bar{\alpha}\bar{\sigma}\bar{\mathbf{u}} - \partial_s\bar{\gamma}\bar{\sigma}\bar{\mathbf{v}} + \mathbf{c}_{-1}) = 0, \tag{35c}$$

$$\bar{\boldsymbol{\eta}}(-\partial_s\bar{\alpha}\bar{\sigma}\bar{\mathbf{u}} - \partial_s\bar{\gamma}\bar{\sigma}\bar{\mathbf{v}} + \mathbf{c}_{-1}) = 0, \tag{35d}$$

from which the slow evolution obtained is

$$\partial_s\alpha = \frac{\mathrm{i}\omega^2}{\sqrt{4-\omega^2}}\gamma(s), \tag{36a}$$

$$\partial_s\bar{\alpha} = -\frac{\mathrm{i}\omega^2}{\sqrt{4-\omega^2}}\bar{\gamma}(s), \tag{36b}$$

$$\partial_s\gamma = -\frac{\mathrm{i}\omega^2}{\sqrt{4-\omega^2}}\alpha(s), \tag{36c}$$

$$\partial_s\bar{\gamma} = \frac{\mathrm{i}\omega^2}{\sqrt{4-\omega^2}}\bar{\alpha}(s). \tag{36d}$$

Now let

$$\alpha(s) = a(s) + \mathrm{i}b(s) \tag{37a}$$

$$\gamma(s) = c(s) + \mathrm{i}d(s) \tag{37b}$$

with a, b, c, d real functions of s. Then,

$$\partial_s\alpha = \partial_s a + \mathrm{i}\partial_s b,$$

$$\partial_s\gamma = \partial_s c + \mathrm{i}\partial_s d.$$

Substituting Eqs. (37) into Eqs. (36) for $0 < \omega < 2$, we obtain

$$\partial_s a = -\frac{\omega^2}{\sqrt{4-\omega^2}}d(s), \tag{38a}$$

$$\partial_s b = \frac{\omega^2}{\sqrt{4-\omega^2}}c(s), \tag{38b}$$

$$\partial_s c = \frac{\omega^2}{\sqrt{4-\omega^2}}b(s), \tag{38c}$$

$$\partial_s d = -\frac{\omega^2}{\sqrt{4-\omega^2}}a(s). \tag{38d}$$

Eqs. (38) have a four-dimensional phase space. Starting from random initial conditions, trajectories are observed to go to infinity as $s \to \pm\infty$. The growing solution for $s \to -\infty$

represents a decaying wave as $s \to \infty$, and vice versa. We expect two-dimensional invariant subspaces, one containing solutions growing as $s \to +\infty$ (unstable subspace) and the other containing solutions growing as $s \to -\infty$ (stable subspace).

The invariant subspaces can be obtained as follows. Putting $d = -a$ and $c = b$ in Eqs. (38), we obtain

$$\partial_s a = \frac{\omega^2}{\sqrt{4-\omega^2}} a(s), \tag{39a}$$

$$\partial_s b = \frac{\omega^2}{\sqrt{4-\omega^2}} b(s), \tag{39b}$$

which shows exponential growth as $s \to +\infty$. This gives the unstable subspace. Similarly putting $d = a$ and $c = -b$, we obtain

$$\partial_s a = -\frac{\omega^2}{\sqrt{4-\omega^2}} a(s), \tag{40a}$$

$$\partial_s b = -\frac{\omega^2}{\sqrt{4-\omega^2}} b(s), \tag{40b}$$

which shows exponential growth as $s \to -\infty$. This gives the stable subspace.

For any arbitrary solution not necessarily restricted to the invariant subspace, the amplitude is given by

$$R(s) = \sqrt{X_{n,c}^2 + X_{n,s}^2} = 2|\alpha(s)u_1 + \gamma(s)v_1|. \tag{41}$$

From Eqs. (27),

$$u_1 = \frac{\sqrt{4-\omega^2}\mathrm{i} - \omega}{2\sqrt{1+\omega^2}},$$

$$v_1 = 0.$$

This gives

$$R(s) = 2|u_1|\sqrt{a^2(s) + b^2(s)}. \tag{42}$$

In particular, restricting attention to the stable subspace,

$$\partial_s R = -\frac{\omega^2}{\sqrt{4-\omega^2}} R(s), \tag{43}$$

which gives

$$R = \mathrm{e}^{-\varepsilon\frac{\omega^2}{\sqrt{4-\omega^2}}n} R_0, \tag{44}$$

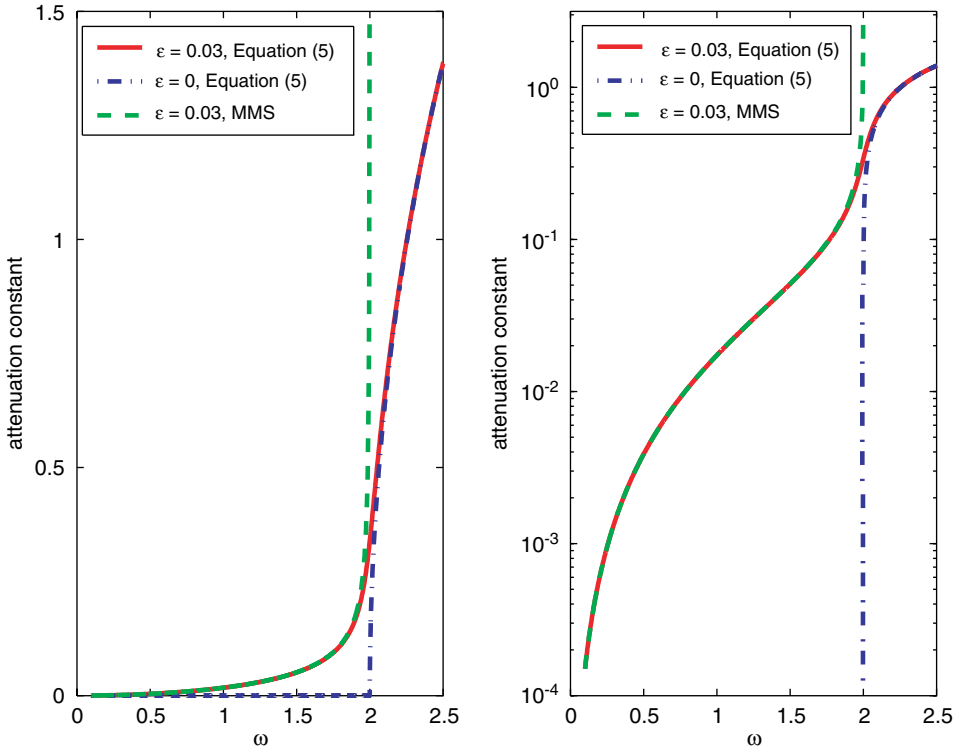

Fig. 4. For the linear structure without damping, the propagation zone (PZ) is $0<\omega<2$. With linear damping ($\varepsilon = 0.03$), the attenuation constants obtained by Eq. (4) and by multiple scales (Eq. (45)) match well.

for some initial amplitude R_0. The attenuation constant is given by

$$Re(\mu) = \frac{\omega^2}{\sqrt{4-\omega^2}}\,\varepsilon \quad \text{for } 0<\omega<2. \tag{45}$$

The attenuation constant obtained from Eq. (4) is compared with that obtained from the above equation in Fig. 4. The match is excellent for ω not very close to 2.

5. MMS for the nonlinearly damped periodic structure

We now consider the weakly and nonlinearly damped periodic structure given by Eq. (7)

$$\mathbf{q}_{n+1} = \mathbf{B}\mathbf{q}_n + \varepsilon \mathbf{N}(\mathbf{q}_n).$$

Applying the MMS as described above, we obtain the following expressions for the slow evolution:

$$\partial_s \alpha = \mathrm{i}C(\omega)(3\gamma^2\bar{\gamma} + 2\alpha\bar{\alpha}\gamma + \alpha^2\bar{\gamma}), \tag{46a}$$

$$\partial_s \bar{\alpha} = -\mathrm{i}C(\omega)(3\gamma\bar{\gamma}^2 + 2\alpha\bar{\alpha}\bar{\gamma} + \bar{\alpha}^2\gamma), \tag{46b}$$

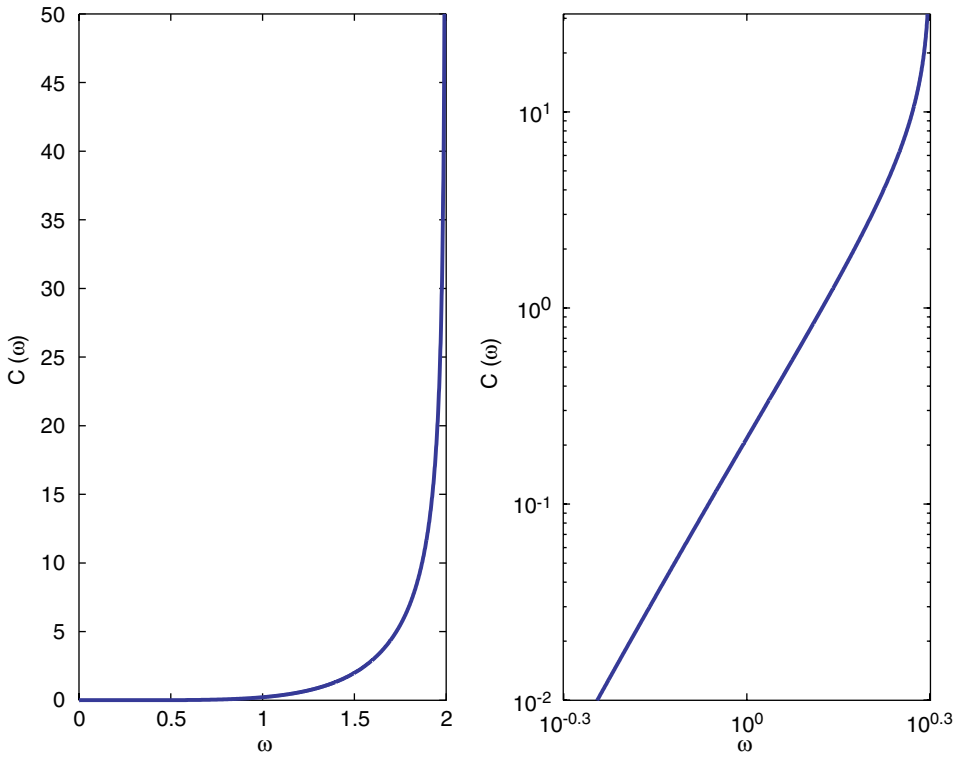

Fig. 5. $C(\omega)$ for $0<\omega<2$.

$$\partial_s\gamma = -\mathrm{i}C(\omega)(3\alpha^2\bar{\alpha} + 2\alpha\bar{\gamma}\gamma + \gamma^2\bar{\alpha}), \tag{46c}$$

$$\partial_s\bar{\gamma} = \mathrm{i}C(\omega)(3\alpha\bar{\alpha}^2 + 2\bar{\alpha}\bar{\gamma}\gamma + \bar{\gamma}^2\alpha), \tag{46d}$$

where $C(\omega)$, a positive real number for $0<\omega<2$ (see Fig. 5), is given by

$$C(\omega) = -\frac{3}{4}\mathrm{i}\frac{\omega^5}{(\omega^4 - 3\omega^2 - 4)}\frac{(\omega^4 - 4\omega^2 + \mathrm{i}\omega\sqrt{4-\omega^2}(2-\omega^2))}{(\omega^2 - \mathrm{i}\omega\sqrt{4-\omega^2} - 2)}. \tag{47}$$

Again putting

$$\alpha(s) = a(s) + \mathrm{i}b(s),$$

$$\gamma(s) = c(s) + \mathrm{i}d(s)$$

in Eq. (46), we obtain

$$\partial_s a = -C(\omega)\left(3d\left(\frac{a^2}{3} + b^2 + c^2 + d^2\right) + 2abc\right), \tag{48a}$$

$$\partial_s b = C(\omega)\left(3c\left(a^2 + \frac{b^2}{3} + c^2 + d^2\right) + 2abd\right), \tag{48b}$$

$$\partial_s c = C(\omega)\left(3b\left(a^2 + b^2 + \frac{c^2}{3} + d^2\right) + 2acd\right), \tag{48c}$$

$$\partial_s d = -C(\omega)\left(3a\left(a^2 + b^2 + c^2 + \frac{d^2}{3}\right) + 2bcd\right). \tag{48d}$$

Eqs. (48) have a four-dimensional phase space. As for the linearly damped case, stable and unstable invariant manifolds can be easily found for this case as well (details omitted).

6. Numerical simulation

For numerical simulation, as shown in Fig. 6, an N-mass periodic structure with fixed-free end conditions is used. The first mass is excited sinusoidally. The equations of motion are as follows. For the first mass,

$$m\ddot{X}_1 = k(X_2 - 2X_1) + \varepsilon(\dot{X}_2 - \dot{X}_1)^r + F\sin(\omega t), \tag{49a}$$

where $r = 1$ for linear damping and $r = 3$ for nonlinear (cubic) damping. For $n = 2$ to $N - 1$,

$$m\ddot{X}_n = k(X_{n+1} + X_{n-1} - 2X_n) + \varepsilon\{(\dot{X}_{n+1} - \dot{X}_n)^r - (\dot{X}_n - \dot{X}_{n-1})^r\}. \tag{49b}$$

For the last mass,

$$m\ddot{X}_N = k(X_{N-1} - X_N) - \varepsilon(\dot{X}_N - \dot{X}_{N-1})^r. \tag{49c}$$

Parameter values used in the simulation are $\omega = \frac{4}{5}$, $\varepsilon = 0.01$, $k = 1$ and $m = 1$. We use $F = 2$ for $N = 1000$ and $F = 5$ for $N = 300$.

6.1. Linear damping

Eq. (49) can be cast in the following matrix form:

$$\mathbf{M}\ddot{\mathbf{X}} + \mathbf{C}\dot{\mathbf{X}} + \mathbf{K}\mathbf{X} = \mathbf{u}\sin(\omega t), \tag{50}$$

where $\mathbf{X} = \{X_1\ X_2\ \cdots\ X_N\}^{\mathrm{T}}$, $\mathbf{u} = \{F0\cdots0\}^{\mathrm{T}}$, $\mathbf{M}, \mathbf{C}, \mathbf{K}$ are the mass matrix, the damping matrix and the stiffness matrix, respectively. After transients die out, the solution $\mathbf{X}$ oscillates with the forcing frequency ω. Assuming $\mathbf{X} = \mathbf{a}\sin(\omega t) + \mathbf{b}\cos(\omega t)$, we solve for $\mathbf{a}$ and $\mathbf{b}$ in terms of $\mathbf{M}$, $\mathbf{C}$,

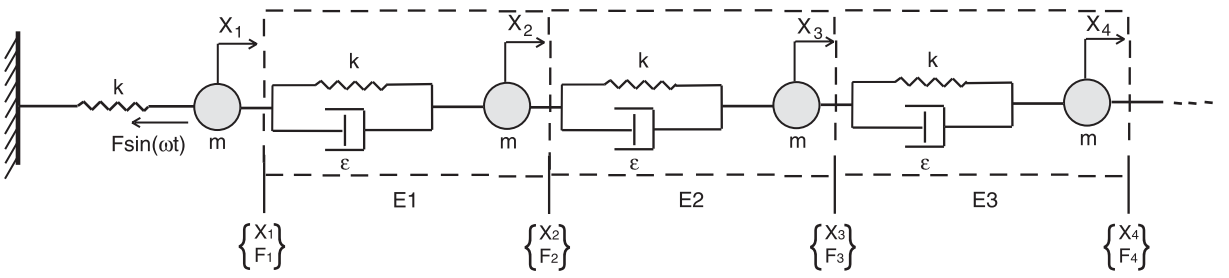

Fig. 6. Periodic structure with the fixed-free end conditions and the first mass excited.

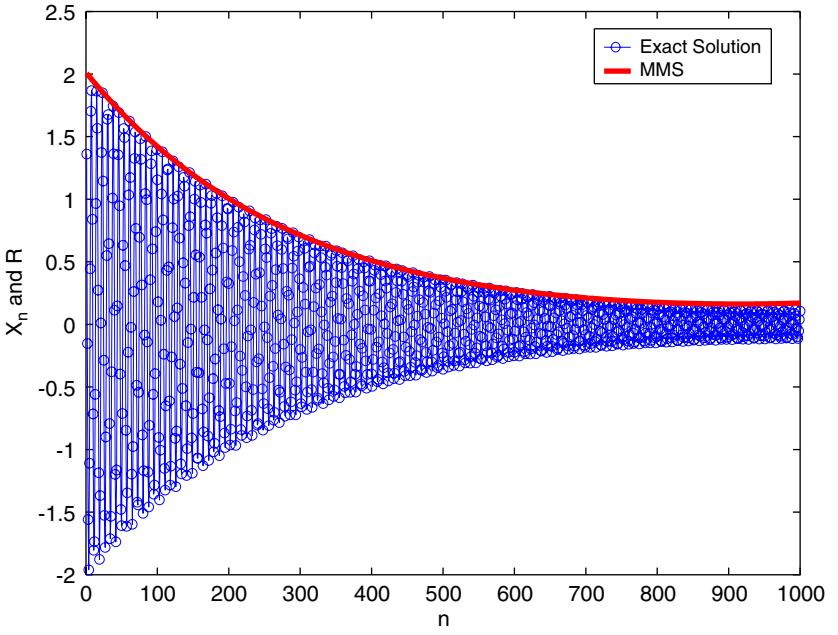

Fig. 7. Linear damping: $N = 1000$, $\varepsilon = 0.01$, $F = 2$ and $\omega = \frac{4}{5}$.

K, **u** and ω. Fig. 7 shows the positions of masses in the steady-state solution at time $t = \pi/2\omega$. Displacements and velocities of the first two masses in the steady state are

$$X_1 = 1.3611, \quad X_2 = -0.153, \quad \dot{X}_1 = 1.177, \quad \dot{X}_2 = 1.591.$$

Substituting the above in the RHS of Eq. (1a) and at $\omega t = \pi/2$, we get

$$X_{1,c} = -1.4712, \quad X_{1,s} = 1.3611, \quad X_{2,c} = -1.9887, \quad X_{2,s} = -0.153.$$

As seen from Fig. 6, we have

$$F_1 = k(X_2 - X_1) + \varepsilon(\dot{X}_2 - \dot{X}_1). \tag{51}$$

Using Eqs. (1), we get

$$F_{1,c} = k(X_{2,c} - X_{1,c}) + \varepsilon\omega(X_{2,s} - X_{1,s}),$$
$$F_{1,s} = k(X_{2,s} - X_{1,s}) + \varepsilon\omega(X_{2,c} - X_{1,c})$$

and substituting numerical values from the above, we get

$$F_{1,c} = -0.5296, \quad F_{1,s} = -1.5099.$$

Now we rewrite Eq. (32) for $n = 1$ in the following manner:

$$\begin{Bmatrix} X_{1,c} \\ X_{1,s} \\ F_{1,c} \\ F_{1,s} \end{Bmatrix} = (a_1 + \mathrm{i}b_1)\begin{Bmatrix} u_1 \\ u_2 \\ u_3 \\ u_4 \end{Bmatrix}\sigma + (c_1 + \mathrm{i}d_1)\begin{Bmatrix} v_1 \\ v_2 \\ v_3 \\ v_4 \end{Bmatrix}\sigma + \text{c.c.},$$

where c.c. denotes complex conjugate of the two terms written. Vectors **u** and **v** are given by Eqs. (27). Solving above equation for a_1, b_1, c_1, d_1, we get

$$a_1 = 0.601, \quad b_1 = 1.1355, \quad c_1 = -1.1323, \quad d_1 = 0.5981.$$

For the MMS results, recall Eqs. (38). Writing

$$\partial_s a \approx \frac{a(s+\varepsilon) - a(s)}{\varepsilon} = \frac{a_{n+1} - a_n}{\varepsilon},$$

$$\partial_s b \approx \frac{b(s+\varepsilon) - b(s)}{\varepsilon} = \frac{b_{n+1} - b_n}{\varepsilon}$$

and likewise for $\partial_s c$ and $\partial_s d$, we convert Eqs. (38) into the map

$$\begin{Bmatrix} a_{n+1} \\ b_{n+1} \\ c_{n+1} \\ d_{n+1} \end{Bmatrix} = \begin{Bmatrix} a_n \\ b_n \\ c_n \\ d_n \end{Bmatrix} - \varepsilon \frac{\omega^2}{\sqrt{4-\omega^2}} \begin{Bmatrix} d_n \\ c_n \\ b_n \\ a_n \end{Bmatrix}. \tag{52}$$

We solve Eq. (52) with the above obtained initial condition. The amplitude is given by (see Eq. (42))

$$R = 2|u_1|\sqrt{a_n^2 + b_n^2}.$$

The match as seen from Fig. 7 is excellent.

6.2. Nonlinear damping

For the nonlinear structure ($r = 3$), a closed-form solution for the steady-state response is not sought here. Eqs. (49) are first integrated numerically using MATLAB's ODE solver (ode45) for some fixed and large number of forcing cycles (here, 5000). This gets rid of initial transients to a large extent, though not completely. The end conditions obtained are used as an initial guess for iterative numerical refinement as follows.

Given an initial guess for the steady state, we integrate for one forcing cycle with high numerical accuracy (in Matlab, the error tolerances were set at 10^{-13}). The difference between the end condition obtained and the initial guess is to be iteratively taken towards zero. The best-known iterative technique is the Newton–Raphson method in which, to seek a zero of $\mathbf{g}(\mathbf{q})$, we let

$$\mathbf{q}_{k+1} = \mathbf{q}_k - [D\mathbf{g}]_{\mathbf{q}_k}^{-1}\, \mathbf{g}(\mathbf{q}_k),$$

where $[D\mathbf{g}]_{\mathbf{q}_k}$ is the Jacobian of $\mathbf{g}$ evaluated at $\mathbf{q}_k$. For arbitrary N-dimensional vector functions of N-dimensional vectors, the Jacobian can be numerically approximated using finite differences, and requires $N+1$ function evaluations (expensive for large N). To speed things up, we can repeatedly use $[D\mathbf{g}]_{\mathbf{q}_0}$ in place of finding $[D\mathbf{g}]_{\mathbf{q}_k}$ each time. The method will still work if the initial guess is good enough; and though a few more iterations may be needed, the total number of function evaluations needed can be much smaller if N is large.

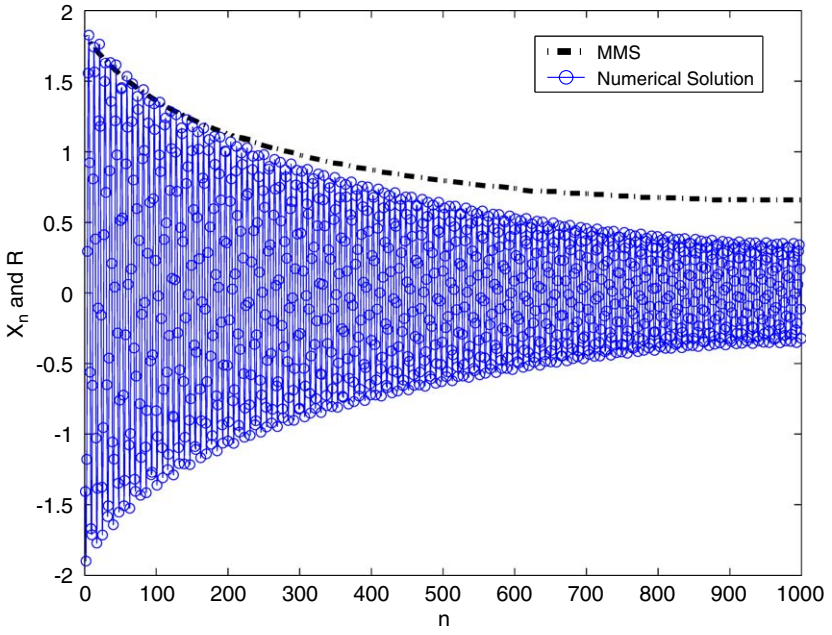

Fig. 8. Nonlinear damping: $N = 1000$, $\varepsilon = 0.01$, $F = 2$ and $\omega = \frac{4}{5}$.

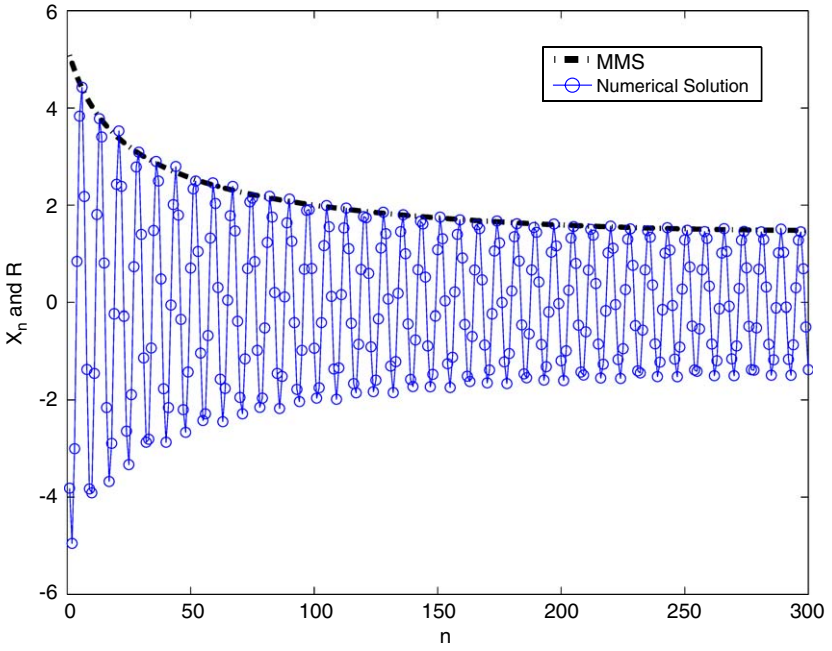

Fig. 9. Nonlinear damping: $N = 300$, $\varepsilon = 0.01$, $F = 5$ and $\omega = \frac{4}{5}$.

The steady-state solutions obtained using the above method are plotted in Fig. 8 for $N = 1000$ and in Fig. 9 for $N = 300$. In Fig. 8, the match is not nearly as good as in the linear damping case; but it is quite good for Fig. 9. This will be discussed below.

To generate the above numerical comparison, we initially proceed exactly as for the linear case. Eq. (48), after converting into a map, gives

$$\begin{Bmatrix} a_{n+1} \\ b_{n+1} \\ c_{n+1} \\ d_{n+1} \end{Bmatrix} = \begin{Bmatrix} a_n \\ b_n \\ c_n \\ d_n \end{Bmatrix} - 4\varepsilon C(\omega) \begin{Bmatrix} 3d_n(\frac{1}{3}a_n^2 + b_n^2 + c_n^2 + d_n^2) + 2a_n b_n c_n \\ -3c_n(a_n^2 + \frac{1}{3}b_n^2 + c_n^2 + d_n^2) + 2a_n b_n d_n \\ 3b_n(a_n^2 + b_n^2 + \frac{1}{3}c_n^2 + d_n^2) + 2a_n c_n d_n \\ 3a_n(a_n^2 + b_n^2 + c_n^2 + \frac{1}{3}d_n^2) + 2b_n c_n d_n \end{Bmatrix}. \tag{53}$$

It remains to iteratively evaluate the map starting from some suitable initial conditions.

We recall that in the MMS, we expand the unknown as

$$\mathbf{q} = \mathbf{Q}_0 + \varepsilon \mathbf{Q}_1 + \cdots,$$

and the MMS then gives the evolution of $\mathbf{Q}_0$. The initial conditions for $\mathbf{Q}_0$ can differ by $\mathcal{O}(\varepsilon)$ from those for $\mathbf{q}$. Keeping this in mind, we used a small, ad hoc, optimization procedure to seek initial conditions for $\mathbf{Q}_0$ that tried to simultaneously keep two things small: (1) the difference between the assumed initial conditions for $\mathbf{Q}_0$ and the numerically obtained initial conditions for $\mathbf{q}$ (see discussion of the linearly damped case), and (2) the difference between the computed final state of $\mathbf{Q}_0$ for the last mass, and the numerically obtained corresponding state $\mathbf{q}$ (this was not done for the linearly damped case).

Note that the details of the optimization procedure and the objective function used[1] are not important for the theory. This is because the MMS tries to find a slow evolution equation whose solutions stay close to the actual solution over n-scales of $\mathcal{O}(1/\varepsilon)$, but which do not necessarily match initial conditions.

The initial guesses provided by the above procedure, and used to generate the figures, are

$$a_1 = 1.7690, \quad b_1 = 2.7321, \quad c_1 = -2.5855, \quad d_1 = 1.8218$$

for $N = 300$ and

$$a_1 = -1.2164, \quad b_1 = 0.3697, \quad c_1 = -0.1679, \quad d_1 = -1.2442$$

for $N = 1000$.

The above results show that for the nonlinear damping case, the MMS does not accurately predict the attenuation over very large numbers of periods of the structure. This should not, however, be viewed as a failure of the method. The basic theorems on the MMS guarantee validity over time scales (or, more appropriately here, n-scales) of $\mathcal{O}(1/\varepsilon)$. Occasionally, as was observed for the linearly damped case, good agreement is obtained over much longer time scales. However, noting that we used $\varepsilon = 0.01$, we expect good agreement over a few hundred periods of the structure but are not surprised if agreement becomes poor over a thousand periods.

[1]We used a weighted sum of the two difference magnitudes (norms).

7. Conclusions

We have studied harmonic wave attenuation in periodic structures with weak damping (both linear and nonlinear). The damping strength was governed by a small parameter ε. The problem was studied using maps which were slightly perturbed versions of simpler maps which had a pair of pure imaginary eigenvalues. These maps were analyzed using the method of multiple scales (MMS), which has so far not been used for such problems. Good agreement between the MMS approximation and full numerics was observed for both cases, when the number of periods of the structure was $\mathcal{O}(1/\varepsilon)$. For the linear damping case, agreement was in fact good for even greater numbers of periods; this is consistent with the fact that the estimate of the attenuation constant, which can be analytically obtained for the linearly damped case, was also very good.

The method presented here can in principle be extended to more complex structures.

Acknowledgements

We acknowledge partial support from ISRO, through the Nonlinear Studies Group at IISc. We thank an anonymous reviewer who prompted us to investigate the match between MMS and numerics, for the nonlinearly damped case, more carefully.

References

[1] D.J. Mead, Wave propagation in continuous periodic structures: research contributions from Southampton, 1964–1995, *Journal of Sound and Vibration* 190 (3) (1996) 495–524.
[2] Y. Yong, Y.K. Lin, Propagation of decaying waves in periodic and piecewise periodic structures of finite length, *Journal of Sound and Vibration* 129 (2) (1989) 99–118.
[3] R.S. Langley, The response of two-dimensional periodic structures to impulsive point loading, *Journal of Sound and Vibration* 201 (2) (1997) 235–253.
[4] E. Rebillard, T. Loyau, J.L. Guyader, Experimental study of periodic lattice of plates, *Journal of Sound and Vibration* 204 (2) (1997) 377–380.
[5] H. Benaroya, Waves in periodic structures with imperfections, *Composites Part B* 28 (1997) 143–152.
[6] D. Wang, C. Zhou, J. Rong, Free and forced vibration of repetitive structures, *International Journal of Solids and Structures* 40 (2003) 5477–5494.
[7] G. Chakraborty, A.K. Mallik, Dynamics of a weakly non-linear periodic chain, *International Journal of Non-Linear Mechanics* 36 (2001) 375–389.
[8] F.C. Hoppensteadt, W.L. Miranker, Multitime methods for systems of difference equations, *Studies in Applied Mathematics* 56 (1977) 273–289.
[9] R. Subramanian, A. Krishnan, Nonlinear discrete time systems analysis by multiple time perturbation techniques, *Journal of Sound and Vibration* 63 (3) (1979) 325–335.
[10] M.H. Holmes, *Introduction to Perturbation Methods*, Springer, New York, 1995.